

Data Fusion and Nonlinear Optimization

By *L. Fatone, P. Maponi, and F. Zirilli*

The practice of collecting data at a scene from multiple sensors of different types results in extremely large amounts of data and has led to the emergence of the research area known as “data fusion.”

Data fusion has been defined [10] as a “formal framework in which are expressed means and tools for the alliance of data of the same scene originating from different sources. It aims at obtaining information of greater quality; the exact definition of greater quality will depend upon the application.” Within the general category of data fusion is image fusion, which van Genderen and Pohl [7] describe as the “combination of two or more different images (of the same scene) to form a new image by using a certain algorithm.”

In the images considered, different quantities are measured, relative to the same scene, by different sensors. To reconstruct these quantities, we can invert the data collected by each sensor, ignoring the other available data, or we can invert all the data collected by the different sensors together. The first approach corresponds to the solution of an inverse problem, while the second corresponds to the “joint” solution of several inverse problems—that is, to a fusion approach. A fusion approach is an attempt to obtain from the available data set higher-quality information about a scene than can be obtained by inversion of the data from the individual sensors, one by one.

The use of data fusion techniques has become common in many application fields, including remote sensing [7], medical imaging [5], and, more generally, inverse scattering problems [3]. In the engineering literature, several fusion approaches have been suggested and developed for improving the quality and accuracy of the information obtained from a given data set; a general survey of the field can be found in [8] and the references therein. If we restrict our attention to remote sensing, Pohl and van Genderen [7] have summarized the most commonly used methods for data fusion.

Data fusion has attracted the interest of the mathematical community in recent years and can be regarded today as a promising chapter of the emerging area of applied mathematics called “image science.” The key factors responsible for this interest are the following: (i) Most scientific data today are digitized, which makes possible, for example, the representation of an image as a matrix of numbers. (ii) The process of measuring an unknown quantity in a scene with a sensor can be modeled by and translated into a set of mathematical relations (usually integral equations) between the measured quantity and the measured data. This is the case in remote sensing, in the use of radar to measure the reflectivity of a scene, or in medical imaging, in the use of computed tomography to measure the mass density of human tissue.

Inverse problems are an established but still flourishing research area in mathematics. We restrict our attention here mainly to linear inverse problems, in which the relation between the unknown and the data is usually represented by a linear equation in an infinite-dimensional Hilbert (or Banach) space.

The main characteristic of linear inverse problems is their ill-posedness—that is, the linear operators in the corresponding linear equations are injective (i.e., they are invertible), although their inverse operators are not bounded. In the processing of real data, which contain errors, the ill-posedness of these problems is a source of difficulty. A naive approach can start from arbitrarily “good” data and produce an arbitrarily “bad” answer. To handle these difficulties, the mathematical literature suggests the use of regularization techniques, such as Tichonov regularization [1].

In this article we present a set of ideas for translating the “joint” solution of several linear (or nonlinear) inverse problems into the solution of a nonlinear (possibly constrained) optimization problem. Such a formulation of data fusion problems leads to challenging optimization problems, as explained later in this article. We present two examples: a remote sensing application and an inverse scattering problem in which the ideas described here are used, beginning from experimental data, to produce interesting results.

A Model Fusion Problem

We propose a data fusion methodology for merging two (or more) data sets relative to a scene, based on the assumption that the unknowns to be determined have in common something that we call “structure.” This assumption is justified by the fact that the unknowns are relative to the same scene. This approach has been considered in the scientific literature; see, for example, [3] and [4].

The term “structure” can be defined in several ways. In general, we define structure as a change in the unknown measured quantities with position in the scene. In this way, two (unknown) quantities are said to have a common structure if they change at the same physical locations. Our approach to the fusion of two data sets is to define an objective function that quantifies the difference in structure between the two unknown (measured) quantities, and then to minimize this objective function subject to a suitable form of the data constraints.

Let \mathbb{R} be the set of real numbers; \mathbb{R}^N , $N > 1$, the N -dimensional real Euclidean space, and \mathbb{C} the set of complex numbers. Let $\Omega \subset \mathbb{R}^2$ be an open set containing the scene being observed. We consider the measurement procedure associated with two sensors,

or more generally with two physical experiments, represented by the equations:

$$F_i(m_i) = u_i, i = 1, 2, \quad (1)$$

where $F_i, i = 1, 2$, are operators that model the measurement processes (i.e., linear or nonlinear operators representing the physical experiments); $m_i : \Omega \rightarrow \mathbb{R}$ (or \mathbb{C}), $i = 1, 2$, are the real (or complex) physical quantities measured by the sensors (i.e., the unknowns of the problem); and $u_i, i = 1, 2$, are the data obtained from the experiments (i.e., the measured data that we call images when u_1, u_2 are functions defined on a subset of \mathbb{R}^2). The data, an estimate of the error affecting them, and the operators used to model the experiments are assumed to be known. As mentioned earlier, the equations in (1) are usually linear equations in infinite-dimensional spaces.

It is easy to see that what follows can be generalized to more than two experiments (i.e., equations). The approach described here, however, is of practical value only for moderate numbers of experiments.

For $i = 1, 2$ the inverse problem consists of determining the unknown m_i when the data u_i and the mathematical model of the physical experiment (i.e., the operator F_i) are known. The simplest approach to reconstruction of the unknowns $m_i, i = 1, 2$, is to solve the corresponding equation (1), inverting, if possible, the operators $F_i, i = 1, 2$. In this way, the two data sets are inverted individually, and the fact that the two equations (1) refer to the same scene is ignored.

A fusion procedure, by contrast, attempts to exploit this last fact. Because the two quantities u_1, u_2 refer to the same scene, we assume that the corresponding m_1 and m_2 have in common the characteristic we call structure; that is, for $i = 1, 2$ there exists an operator S_i , to be modeled, that maps m_i in the structure $S_i(m_i)$ associated with m_i . When m_1 and m_2 refer to the same scene, we assume that $S_1(m_1) = S_2(m_2)$. The structure operators $S_i, i = 1, 2$, can be defined in many different ways, most commonly as follows:

■ If there exists a known functional relation between m_1 and m_2 , for example $m_1 = \psi(m_2)$ for some known function ψ , then we can state that $S_1(m_1) = m_1$ and $S_2(m_2) = \psi(m_2)$.

■ If the functions $m_i, i = 1, 2$, are piecewise-constant and change in the same locations, then $S_i(m_i)$ can be defined as the characteristic function of the support of $\nabla m_i, i = 1, 2$, where $\nabla \cdot$ denotes the gradient of \cdot .

A measure of the difference in structure between m_1 and m_2 can be defined as follows:

$$\phi = \|\|S_1(m_1) - S_2(m_2)\|\|^2, \quad (2)$$

where $\|\| \cdot \|\|$ is a suitable norm of \cdot , so that a possible approach to the joint inversion of (1) is to solve the following optimization problem: Given $\varepsilon > 0$,

$$\underset{m_1, m_2}{\text{minimize}} \{ \|\|S_1(m_1) - S_2(m_2)\|\|^2 + G(m_1, m_2) \} \quad (3)$$

subject to the constraint:

$$\|\|F_1(m_1) - u_1\|\|^2 + \|\|F_2(m_2) - u_2\|\|^2 \leq \varepsilon^2. \quad (4)$$

The real function $G(m_1, m_2)$ in (3) is a penalty term containing a priori information about the desired solution eventually available. In (4) the parameter ε is a target misfit; its value depends on the errors present in the data.

The nonlinear optimization problem (3), (4) is only one example of the translation of a data fusion problem into mathematical terms. Other variations of this problem can be investigated, and, consequently, other ad hoc optimization problems can be formulated. Special algorithms can be designed for the numerical solution of the proposed optimization problems. In fact, we expect problem (3), (4) and its variations to be challenging optimization problems. The operators S_1, S_2 in (3) are usually highly nonlinear, and the discretized version of the unknowns m_1, m_2 can lead to finite-dimensional optimization problems involving hundreds of thousands, if not millions, of independent variables. The ill-posedness of (1) and, consequently, of the constraint (4) combines with the highly nonlinear character of the objective function (3) and the huge number of independent variables in the discretized version of problem (3), (4) to produce a very difficult optimization problem.

Optimization Problems in Image Fusion: SAR/Optical Image Fusion

Remotely sensed images obtained by sensors traveling on satellites have proved to be of great interest to those responsible for assessing the Earth's resources and monitoring the environment. This is so because the large amounts of data acquired by sensors of different types provide repeated coverage of the planet on a regular basis. Efficient exploitation of these data requires the development of effective data fusion techniques that can take advantage of the multisource and multitemporal nature of the data.

We limit our attention here to an example of image fusion in remote sensing: the combination of images from optical and SAR (Synthetic Aperture Radar) sensors relative to the same scene on the Earth's surface to achieve better information-extraction capabilities over features of interest in the observed scene.

The optical data measure the reflectivity of the ground cover in the visible and near-infrared spectrum (i.e., the luminance of the scene). The SAR data measure the reflectivity in the microwave spectrum (i.e., the backscattering coefficient) and are very sensitive

to the shape, orientation, roughness, and moisture content of the illuminated objects on the ground. The wavelength of the radiation used by microwave sensors is much longer than that used by optical sensors. Because optical and SAR imaging systems have different physics, they have a potential for complementarity and data fusion.

In this case, in (1) u_1, u_2 represent the SAR and optical images, respectively; m_1, m_2 are the corresponding reflectivity and luminance of the scene; F_1 and F_2 represent the SAR and the optical image measurement simulators that, for simplicity, we assume later to be the identity operators. The images u_1, u_2 are regarded as real functions defined on a rectangular region Ω of \mathbb{R}^2 , discretized on the rectangular grid given by the usual pixel structure of the images.

Because F_1, F_2 are chosen to be the identity operators, the basic assumption requiring that the reflectivity and the luminance of the scene be piecewise-constant functions that change in the same physical locations is made directly on the SAR and optical images. This assumption is amply fulfilled in practice. When F_1 and F_2 are the identity operators, the output of the fusion procedure described in the previous section is two images (corresponding to the original SAR and the original optical image, respectively) of the same type but (we hope) of higher quality than those used as data. In other words, we essentially perform a fusion of data without jointly inverting equations (1), which, in fact, reduce in this case to trivial equations.

Specifically, given two real-valued functions defined on $\Omega \subset \mathbb{R}^2$, we obtain the fused images s_1^+, s_2^+ as the minimizer of the following nonlinear optimization problem:

$$\underset{s_1, s_2}{\text{minimize}} \{ \| \| S_1(s_1) - S_2(s_2) \| \|^2 + G(s_1, s_2) \}, \quad (5)$$

where the penalty term $G(s_1, s_2)$ is chosen as follows:

$$G(s_1, s_2) = \lambda_1 \| \| s_1 - u_1 \| \|^2 + \lambda_2 \| \| s_2 - u_2 \| \|^2, \quad (6)$$

and the parameters $\lambda_i, i = 1, 2$, are suitable positive penalty constants. In this case $S_i(s_i) = S_{\tau_1, \tau_2}(\| \nabla s_i \|)$, $i = 1, 2$, where $\| \cdot \|$ is the Euclidean norm in \mathbb{R}^2 and $S_{\tau_1, \tau_2}(\cdot)$ is a smoothed version of a suitable step function depending on the parameters τ_1, τ_2 . In particular, the function S_{τ_1, τ_2} is such that we have $\tau_1 < \tau_2$, $S_{\tau_1, \tau_2}(\xi) = 0$ for $\xi < \tau_1$ and $S_{\tau_1, \tau_2}(\xi) = 1$ for $\xi > \tau_2$; moreover, we require S_{τ_1, τ_2} to be differentiable and monotone. Finally $\tilde{s}_i, i = 1, 2$, is a smooth approximation with steep gradients of the piecewise-constant functions $s_i, i = 1, 2$. That is, $S_i(s_i), i = 1, 2$, is an approximation of the characteristic function of the support of $\nabla s_i, i = 1, 2$.

If s_1^+, s_2^+ is the solution of the optimization problem (5), (6), then s_1^+ is the ‘‘fused image’’ that replaces the measured SAR image u_1 and, similarly, s_2^+ is the ‘‘fused image’’ that replaces the measured optical image u_2 . Because $F_1 = F_2 = \text{identity operator}$, the data constraint is already contained in the penalty term (6) and the constraint (4) is omitted in this case. The behavior of the fusion procedure described earlier depends on the values of the parameters $\tau_i, \lambda_i, i = 1, 2$. Careful calibration of these parameters is necessary, depending on the characteristics of the images to be treated.

In Figure 1 we present numerical results obtained from real SAR and optical images of an agricultural/forest/peri-urban landscape, north of Paris, that includes a part of the Roissy Charles de Gaulle airport. The optical and SAR data used for the experiment are SPOT and ERS data, respectively. The data were provided by SPOT Image, a partner in this project. Each image contains 190×190 pixels and is mono-channel, with 20-meter resolution, orthorectified with a Digital Elevation Model (DEM) of the observed scene. In this case problem (5), (6), when discretized using the pixel structure of the images, has $2 \times 190 \times 190 = 72,200$ independent variables and has been solved with the optimization software package LANCELOT (see [2]).

Inspection of Figure 1 shows that the information contained in the fused images is of higher quality than that provided by the original images; the improved quality can be seen, for example, in the straight lines contained in the images.

An Image Fusion Approach to An Inverse Scattering Problem

The data fusion approach described in the print version of this article was also used in a second prob-

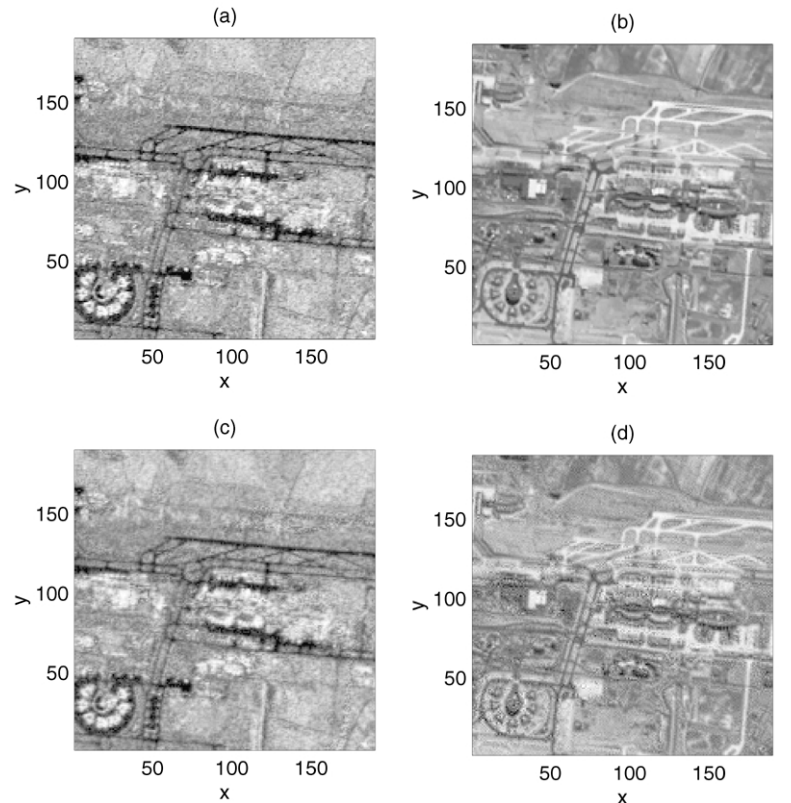


Figure 1. Original SAR (a) and optical (b) images, and fused SAR (c) and optical (d) images. The unit in the x and y direction is given by the corresponding pixel size (1 pixel = 20m x 20m). The white areas represent high values (gray level = 255) and the black areas low values (gray level = 0) of the pixel variable.

lem: the numerical inversion of electromagnetic scattering data at different frequencies (see [3]) collected at a scene in a laboratory experiment. This multifrequency inverse scattering problem can be formulated more precisely as follows: Reconstruct the refraction index of a cylindrically symmetric (along the z -axis) inhomogeneity from some knowledge of the scattered electromagnetic waves arising from the interaction of the inhomogeneity with known incident electromagnetic waves (see Figure 2).

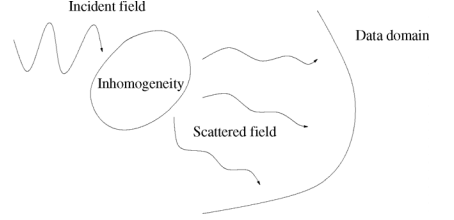


Figure 2. *The inverse scattering problem.*

The incident electromagnetic waves are time-harmonic plane waves linearly polarized along the axis of symmetry of the cylindrical inhomogeneity. We assume that the cross section of a cylinder containing the inhomogeneity can be chosen to be a compact set of the plane. In that case the electromagnetic scattering problem can be reduced to a problem in two dimensions for a scalar field (see [3], [6]). That is, the observed scene (i.e., the cross section of a rectangular cylinder containing the inhomogeneity) is a compact region of the plane and contains one or several subregions that, in turn, contain the (cross section of the) inhomogeneities used as scatterers when a known incident electromagnetic field of the type described above hits the inhomogeneities. We assume that the refraction indices of the observed scene are unknown functions of the frequency f of the electromagnetic waves used in the scattering experiments. From knowledge of the incoming electromagnetic fields and of the corresponding scattering data (i.e., the electric far fields) at different frequencies, we want to reconstruct the refraction indices of the scene at the frequencies used in the experiments.

The scattered data collected at each frequency form a data set. These data sets can be inverted either one by one or jointly, in a data fusion procedure. The basic underlying assumption in the fusion procedure is that the refraction indices of the scene at the different frequencies are piecewise-constant functions and that their gradients have the same support.

For $i = 1, 2$ we define $m_{k_i}(\mathbf{y}) = 1 - n_{k_i}(\mathbf{y})$, where $n_{k_i}(\mathbf{y})$ is the refraction index of the scene considered as a function of the location in the scene $\mathbf{y} \subset \mathbb{R}^2$ and of the wave number k_i (corresponding to the frequency $f = f_i$ considered), and the data u_{k_i} are the scattered electric far fields generated when the inhomogeneity is hit by the incoming electromagnetic plane wave $u_{k_i}^i$. For $i = 1, 2$ in the Born approximation, the operator F_{k_i} , which models the measurement process, is expressed by a Fredholm integral operator of the first kind. That is, the equations (1) are of the form:

The scattered data collected at each frequency form a data set. These data sets can be inverted either one by one or jointly, in a data fusion procedure. The basic underlying assumption in the fusion procedure is that the refraction indices of the scene at the different frequencies are piecewise-constant functions and that their gradients have the same support.

$$u_{k_i}(\hat{\mathbf{x}}, \hat{\alpha}) = -\frac{k_i^{3/2}}{\sqrt{8\pi}} e^{i\pi/4} \int_B m_{k_i}(\mathbf{y}) e^{-ik_i(\hat{\mathbf{x}} \cdot \mathbf{y})} u_{k_i}^i(\mathbf{y}, \hat{\alpha}) d\mathbf{y}, \quad (7)$$

$$\hat{\mathbf{x}}, \hat{\alpha} \in \mathbf{S}_1, \quad i = 1, 2,$$

where i is the imaginary unit, $\hat{\mathbf{x}} = \hat{\mathbf{x}} / \|\hat{\mathbf{x}}\|$, $\hat{\mathbf{x}} \neq \mathbf{0}$ and $\hat{\alpha}$, with $\|\hat{\alpha}\| = 1$, is the direction in which the plane wave $u_{k_i}^i$ propagates. $\langle \cdot, \cdot \rangle$ is the Euclidean scalar product.

Comparing equations (1) with equations (7), for $i = 1, 2$, we identify the two unknowns m_i with the quantities $m_{k_i} = 1 - n_{k_i}$, the data u_i with the electric far fields $u_{k_i}(\hat{\mathbf{x}}, \hat{\alpha})$, and the operators F_i with the integral operators defined on the right-hand side of formula (7).

With these correspondences in mind, we solved the constrained optimization problem (3), (4), taking $S_i(m_{k_i}) = S_{\tau_1, \tau_2}(\|\nabla \tilde{m}_{k_i}\|)$, $i = 1, 2$ (where \tilde{m}_{k_i} , $i = 1, 2$, is a smooth approximation of m_{k_i} , $i = 1, 2$) as structure operators and choosing the penalty term $G(\cdot, \cdot)$ in (3) as follows:

$$G(m_{k_1}, m_{k_2}) = \lambda_1 \|m_{k_1} - m_{k_1}^*\|^2 + \lambda_2 \|m_{k_2} - m_{k_2}^*\|^2. \quad (8)$$

In (8) λ_i , $i = 1, 2$, are suitable positive penalty parameters and $m_{k_i}^*$, $i = 1, 2$, are two approximations of the unknowns obtained in the separate solution of the two equations (7) for $k = k_1$ and $k = k_2$, respectively—that is, the solution of two distinct single-frequency inverse scattering problems by the procedure presented in [6]. The integral equations (7) are ill-posed.

The fusion procedure proposed has been tested on experimental data provided by the Institut Fresnel, CNRS, Marseille, France. We used the software package LANCELOT (see [2]) to obtain the numerical results presented in Figure 3, with $k = 83.83\text{m}^{-1}$ and $k_2 = 167.67\text{m}^{-1}$ as wave numbers in the fusion problem. The inhomogeneity is a metallic “U”-shaped target, made from a $0.08\text{m} \times 0.05\text{m}$ rectangle with a rectangular ($0.075\text{m} \times 0.04\text{m}$) cavity. Because the target is metallic, we are outside the region of validity of the Born approximation. Nevertheless, the inversion procedure described in this article seems to work reasonably well. The obstacle is contained in an $r \times r$ square ($r = 0.1\text{m}$), and the unknowns m_{k_1} , m_{k_2} are approximated by piecewise-constant functions on the uniform rectangular grid in which $r = 0.1\text{m}$ and in which there are $N = 64$ rectangular grid elements in each coordinate direction. The resulting optimization problem has $4 \times 64 \times 64 = 16,384$ independent variables.

In Figure 3, $m_{k_1}^+$, $m_{k_2}^+$ represent the “fused” images, i.e., the minimizer that is the solution to the optimization problem that models the fusion procedure.

The numerical results obtained with the proposed fusion procedure show accurate reconstructions of the inhomogeneity. The presence of nontrivial simulators F_i , $i = 1, 2$, in the fusion problem (3), (4) and their ill-posedness make difficult the use of large numbers of independent variables in the discretized problem.

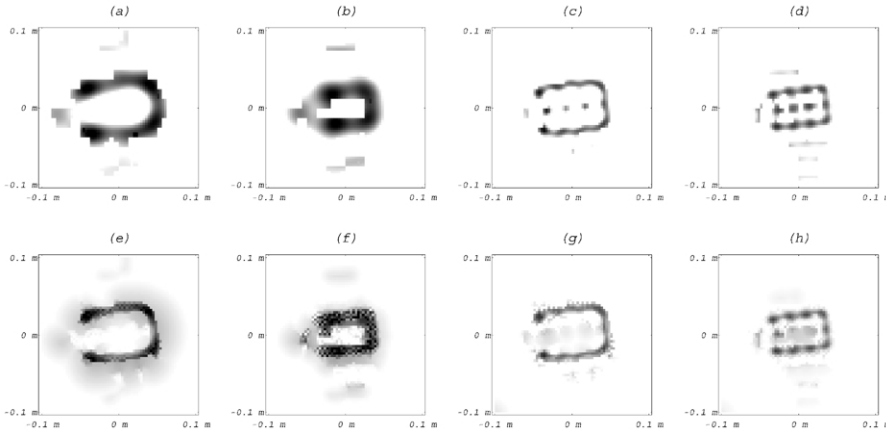


Figure 3. (a) The real part of $m_{k_1}^*$, (b) the imaginary part of $m_{k_1}^*$, (c) the real part of $m_{k_2}^*$, (d) the imaginary part of $m_{k_2}^*$, (e) the real part of $m_{k_1}^*$, (f) the imaginary part of $m_{k_1}^*$, (g) the real part of $m_{k_2}^*$, (h) the imaginary part of $m_{k_2}^*$. The real parts range from -103.35 to 0 , and the imaginary parts from -152.66 to 0 , on a linear gray-scale that associates black with lower numbers and white with higher numbers. Units in the x and y directions are meters.

blems now under investigation in the fusion community: (i) identification of fusion procedures of practical value when huge numbers of images of the same scene must be fused, and (ii) definition in mathematical terms of the “higher quality” sought in fused images as compared with the original images used in the fusion procedure.

References

- [1] D. Colton and R. Kress, *Inverse Acoustic and Electromagnetic Scattering Theory*, Springer-Verlag, Berlin, 1992.
- [2] A.R. Conn, N.I.M. Gould, and P.L. Toint, *LANCELOT: A Fortran Package for Large Scale Nonlinear Optimization (Release A)*, Springer-Verlag, Berlin, 1992.
- [3] L. Fatone, P. Maponi, and F. Zirilli, *An image fusion approach to the numerical inversion of multifrequency electromagnetic scattering data*, submitted to *Inverse Problems*, 17 (2001), 1689–1701.
- [4] E. Haber and D. Oldenburg, *Joint inversion: A structural approach*, *Inverse Problems*, 13 (1997), 63–77.
- [5] K. Kneöaurek, M. Ivanovic, J. Machac, and D.A. Weber, *Medical image registration*, *Europhysics News*, 31 (2000), 5–8.
- [6] P. Maponi, L. Misici, and F. Zirilli, *A numerical method to solve the inverse medium problem: An application to the Ipswich data*, *IEEE Antennas and Propagation magazine*, 39 (1997), 14–19.
- [7] C. Pohl and J.L. van Genderen, *Multisensor image fusion in remote sensing: Concepts, methods and applications*, *Internat. J. Remote Sensing*, 19 (1998), 823–854.
- [8] *Special issue on data fusion*, *Proceedings of the IEEE*, 85 (1997), 1–208.
- [9] A. Quarteroni and A. Valli, *Domain De-composition Methods for Partial Differential Equations*, Oxford Science Publications, 1999.
- [10] L. Wald, *Data fusion: A conceptual approach for an efficient exploitation of remote sensing images*, in *Proceedings of EARSel Conference on Fusion of Earth Data*, T. Ranchin and L. Wald, eds., 1998, 17–23.

Acknowledgments

The partners for the SAR/optical data fusion project described in this article are ESA (ESRIN, Italy) and SPOT Image (France). The research on SAR/optical image fusion has been supported by ESA–ESRIN through ESRIN contract 13796/99/I–DC, “Study of optical/SAR complementarity and data fusion techniques,” awarded to the Università di Camerino, Italy. The authors thank Institut Fresnel (France) for its contribution to this activity. Finally, the authors thank A.R. Conn, N.I.M. Gould, and P.L. Toint for making available, free of charge, the optimization package LANCELOT.

L. Fatone is a research associate in the Dipartimento di Matematica Pura e Applicata at the Università di Modena e Reggio Emilia, Italy. P. Maponi is a research associate in the Dipartimento di Matematica e Fisica at the Università di Camerino, Italy. F. Zirilli is a professor in the Dipartimento di Matematica “G. Castelnuovo,” Università di Roma “La Sapienza.”

Conclusions

The fusion procedures described in this article have proved to be computationally efficient and to yield good results. Because the number of independent variables in the discretized problems can be large, some particular structure—sparsity, for example—must be exploited in the discretized version of the optimization problem.

In the case of images with large numbers of independent variables, one possible idea is to attack the numerical fusion problem by a domain decomposition approach similar to that usually employed in the numerical treatment of PDEs to exploit the computational power of parallel machines (see 8). A second approach is to sparsify, when possible, the discretized version of equations (1) with, for example, wavelets.

We conclude by mentioning two prob-